

Dissolution Kinetics of Phenylbutazone

K. G. MOONEY * §, M. RODRIGUEZ-GAXIOLA ‡, M. MINTUN ‡,
K. J. HIMMELSTEIN ‡, and V. J. STELLA * *

Received August 8, 1980, from the *Department of Pharmaceutical Chemistry and the †Department of Chemical Engineering, University of Kansas, Lawrence, KS 66045. Accepted for publication April 17, 1981. §Present address: Boehringer Ingelheim, Ridgefield, CT 06877.

Abstract □ This study investigated the possible effects of simultaneous, noninstantaneous, reversible chemical ionization of carbon acids on the dissolution of a typical pharmaceutical carbon acid, phenylbutazone, and its deuterio analog. The dissolution rate *versus* pH profile for phenylbutazone was consistent with phenylbutazone acting as if it were an acid where the ionization can be considered instantaneous. In view of the dissolution behavior of phenylbutazone under various conditions, it is unlikely that the noninstantaneous ionization kinetics demonstrated for this compound play a major role in determining the dissolution rate, either *in vitro* or *in vivo*, since the average residence time in a typical aqueous diffusion layer for phenylbutazone dissolution is longer than the reaction time for its ionization. Slowing the reaction time with a primary isotope effect by deuterium substitution for the ionizable proton caused significant deviation from classical behavior for *d*-phenylbutazone.

Keyphrases □ Phenylbutazone—dissolution kinetics □ Kinetics—dissolution phenylbutazone □ Dissolution—kinetics of phenylbutazone □ Anti-inflammatory agents—phenylbutazone, dissolution kinetics

In modeling the dissolution of carboxylic acids into aqueous, alkaline media (1, 2), all reversible ionization reactions occurring in the diffusion layer are considered instantaneous¹. Carbon acids, where the dissociating proton is bound to a carbon atom rather than to a heteroatom, have been shown to undergo noninstantaneous rates of ionization (3–5); *i.e.*, proton abstraction rate constants are considerably slower than $10^{10} M^{-1}/\text{sec}$. The present study investigated the possible effects of simultaneous, noninstantaneous, reversible chemical ionization of carbon acids on the dissolution of phenylbutazone (I).

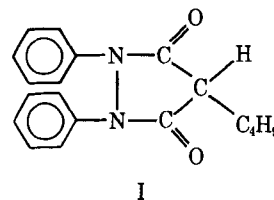
An anti-inflammatory agent, phenylbutazone was chosen because it has been demonstrated to have dissolution rate-limited absorption (6–9) and noninstantaneous ionization kinetics (3). Furthermore, studies on the mass transport of phenylbutazone have described behavior that seemed not entirely explicable by models with the assumption that this drug undergoes instantaneous ionization (10–12).

The pH-stat, rotating-disk system described previously (1) was particularly useful for the study of the phenylbutazone dissolution mechanism in aqueous media of variable bulk solution pH since buffers have been demonstrated to catalyze markedly the rate processes involved in its ionization (3). The inclusion of buffers in the dissolution medium complicates the theoretical considerations of any model and prevents any possible effects of noninstantaneous ionization on phenylbutazone dissolution rates from being observed.

THEORETICAL

The ionization kinetics of phenylbutazone can be described by Schemes I and II and are adapted from the work of Stella and Pipkin (3). In these

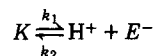
¹ Instantaneous is regarded here in the chemical kinetic sense, in which a reaction rate constant is at or approaches the diffusion-controlled limit of $\sim 2 \times 10^{10} M^{-1}/\text{sec}$.



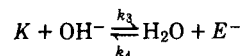
schemes, *K* is the diketo form of phenylbutazone, *E*⁻ is the enolate anion, and OH⁻ and H⁺ represent hydroxide and hydrogen ions, respectively. It was demonstrated (3) that in an aqueous solution of ionic strength (μ) 0.1 and at 25°, an enol form comprises a minor portion of the total undissociated phenylbutazone (~2%). Therefore, it was assumed that solid phenylbutazone exists predominantly as the diketo form, and any ionization during dissolution due to reaction with water and hydroxide ion was regarded as occurring solely from this species.

It was assumed that a previously described (1) diffusion layer model generally applied; the only difference between the previous model and the present one was that chemical reactions involving the diketo or enolate forms of phenylbutazone were assumed to be noninstantaneous with respect to the diffusion process. Phenylbutazone species were not presumed to be in equilibrium with one another at any point within the diffusion layer.

When the bulk solution pH (pH_{bulk}) was maintained only by controlled addition of hydroxide ion from a pH-stat system (1), the various reactions occurring within the diffusion layer were given by Schemes I and II.



Scheme I



Scheme II

Also occurring in the diffusion layer was the spontaneous ionization of water (Scheme III).



Scheme III

At steady state during the dissolution of phenylbutazone, a mass balance for each diffusing species may be written accounting for both chemical ionization reactions and Fickian diffusion within the diffusion layer:

$$\frac{\partial [K]}{\partial t} = D_K \frac{\partial^2 [K]}{\partial X^2} - \left[[K](k_3[\text{OH}^-] + k_1) - [\text{E}^-](k_2[\text{H}^+] + k_4) \right] = 0 \quad (\text{Eq. 1})$$

$$\frac{\partial [\text{E}^-]}{\partial t} = D_E \frac{\partial^2 [\text{E}^-]}{\partial X^2} - \left[[\text{E}^-](k_2[\text{H}^+] + k_4) - [K](k_3[\text{OH}^-] + k_1) \right] = 0 \quad (\text{Eq. 2})$$

$$\frac{\partial [\text{OH}^-]}{\partial t} = D_{\text{OH}} \frac{\partial^2 [\text{OH}^-]}{\partial X^2} - \left[k_3[K][\text{OH}^-] - k_4[\text{E}^-] \right] = 0 \quad (\text{Eq. 3})$$

$$\frac{\partial [\text{H}^+]}{\partial t} = D_H \frac{\partial^2 [\text{H}^+]}{\partial X^2} - \left[k_2[\text{E}^-][\text{H}^+] - k_1[K] \right] = 0 \quad (\text{Eq. 4})$$

where $[K]$, $[\text{E}^-]$, $[\text{OH}^-]$, and $[\text{H}^+]$ represent the concentrations of the various species; D_K , D_E , D_{OH} , and D_H are their diffusivities; t is time; k_{1-4} are the rate constants described in Schemes I and II; and where x is the distance of any point from the solid-liquid interface.

The relationship between $[\text{H}^+]$ and $[\text{OH}^-]$ is defined in the diffusion layer by:

$$K_w = [H^+][OH^-] \quad (\text{Eq. 5})$$

but the relationships between $[K]$ and $[E^-]$ and $[H^+]$ and $[OH^-]$ cannot be given by a series of simple equilibria because of the noninstantaneous nature of the ionization reactions involved. Since the rates of interconversion between K and E^- at any point in the film depended on their respective concentrations and $[H^+]$ and $[OH^-]$ at that position, there was no simple analytical solution of Eqs. 1-4. Therefore, to predict whether the noninstantaneous nature of phenylbutazone ionization was likely to affect the dissolution rate of the acid, numerical integration methods were used with Eqs. 1-4 to provide approximate film concentration profiles for $[K]$ and interfacial pH values, pH_0 , under various pH_{bulk} conditions.

EXPERIMENTAL

Materials—Phenylbutazone² and 2-naphthoic acid³ were obtained in pure crystalline forms. Deuterium oxide³ (99.9 mole % purity), deuterium chloride³ solution (10 M), and sodium deuterioxide³ (40% solution) were all used without further purification. Reagent grade hydrochloric acid⁴ and sodium hydroxide⁴ were obtained as prepared (1 M) solutions. All other chemicals were reagent grade.

Preparation of Deuterated Phenylbutazone and 2-Naphthoic Acid—Deuterated phenylbutazone was prepared by dissolving ~5 g of nondeuterated phenylbutazone in 50 ml of deuterium oxide and 1.0 ml of 40% sodium deuterioxide with vigorous agitation. Upon addition of 1-2 ml of 10 M deuterium chloride, a gel-like precipitate was formed; it was filtered and dried at 50-60° under vacuum for 1-2 hr. After recrystallization in 99.9% deuterated ethanol³ (*d*-ethanol), TLC, using a solvent system of 7% (v/v) acetone in toluene, showed only one spot that corresponded to phenylbutazone.

The melting point of the pure phenylbutazone standard (starting material) was 105-106°, and that of the precipitate prior to recrystallization was 95-106° (transition observed in that range). The polymorphism of phenylbutazone has been well documented(13, 14), and it appeared that the highest melting and, therefore, most thermodynamically stable crystalline form of phenylbutazone, has a melting point of 105-106°. After recrystallization in *d*-ethanol and drying at 50-60° *in vacuo* for 2 hr, deuterated phenylbutazone (*d*-phenylbutazone) gave a sharp melting point of 105-106°. Therefore, it was assumed that the crystalline form of *d*-phenylbutazone was very similar to that of the pure nondeuterated material.

2-Naphthoic acid was deuterated in a similar manner, using approximately the same amounts of solid and reagents. On measuring the melting points of the starting protonated material and the deuterated precipitate, they were 184-185° (lit. mp 185-187°) and 179-181°, respectively. After recrystallization of the precipitated deuterated compound in *d*-ethanol, the melting point of the pure solid was only 180-181°, ~4° lower than the starting material.

IR and NMR spectra were obtained to confirm the deuteration sites in both compounds. Phenylbutazone was deuterated only at the 2-position, with the percentage deuteration being estimated at >90%. Naphthoic acid was similarly deuterated only on the exchangeable carboxy function, the percentage deuteration again being estimated at >90%. Both deuterated compounds were stored in a desiccator until required.

Solubility and pKa Measurement of Phenylbutazone—The aqueous solubility of phenylbutazone at $\mu = 0.5$ (potassium chloride) and 25° was determined as described earlier (1). Additionally, a spectrophotometric method was used to obtain the pKa of phenylbutazone independently. Phenylbutazone showed a strong bathochromic shift at 240-300 nm on addition of base to an aqueous solution of the compound. Thus, aliquots of an approximate 1.3×10^{-5} M aqueous solution of phenylbutazone at $\mu = 0.5$ with potassium chloride were taken and, using 0.1-1.0 M NaOH or HCl, were adjusted to pH values of 2.0-10.0. The absorbance of each solution was measured at 262 nm with a UV-visible spectrometer⁵.

The pKa and intrinsic solubility of 2-naphthoic acid were measured by the solubility method as described previously (1) at 25° and $\mu = 0.5$ (potassium chloride).

Initial Dissolution Rate Measurement as Function of Rotation Speed and pH—Phenylbutazone and 2-naphthoic acid in both their

deuterated and protonated forms were compressed into solid disks of 1.3-cm diameter as described previously (1).

The adherence of the dissolution rate from a rotating disk of constant surface area at a given pH_{bulk} to a diffusion layer-controlled model described by the Levich-Nernst relationship (1) was tested for in all four compounds. Phenylbutazone, 2-naphthoic acid, and deuterated 2-naphthoic acid (*d*-2-naphthoic acid) were tested in a medium of pH_{bulk} 2.00 (0.49 M KCl-0.01 M HCl), $\mu = 0.5$, and 25°. Dissolution rates of phenylbutazone and *d*-phenylbutazone were also measured at pH_{bulk} 6.50 as a function of disk rotation speed, using a pH-stat system to maintain the bulk solution pH constant. To compare phenylbutazone dissolution rates under acidic conditions, the dissolution rates of *d*-phenylbutazone were also measured at 600 rpm under acidic conditions. The method and apparatus used were exactly as described previously (1).

To measure dissolution rate as a function of pH_{bulk} , the solid acid disks were rotated at a constant speed in media of different pH values. For phenylbutazone and *d*-phenylbutazone, the disk rotation speed was 600 rpm; for *d*-2-naphthoic acid and 2-naphthoic acid, it was 450 rpm. The difference was due to the compound's relative solubilities and the period of time required to measure each dissolution rate.

Dissolution Rate Simulations—Where phenylbutazone and/or deuterated phenylbutazone dissolution was simulated, the boundary conditions were defined as follows:

1. At the rotating-disk surface, *i.e.*, $X = 0$, $[K]$ is given by the intrinsic solubility of phenylbutazone, $[HA]_0$.
2. To estimate the boundary condition for $[E^-]$ at the wall, the experimentally observed flux (J_{obs}) was used since it was equal to the sum of K flux, J_K , and E^- flux, J_E , and $[E^-]$ was changed successively until the value for J_{obs} simulated was equal to J_{obs} experimentally observed.
3. To set the boundary condition for $[OH^-]$, it was assumed that at any given point, the $[E^-]$ flux out of the diffusion layer should be equal to the influx of $[OH^-]$ plus the flux of $[H^+]$ out (1) since any change in the flux of $[OH^-]$ must also be reflected by corresponding changes in $[E^-]$ and $[H^+]$. This statement was expressed as:

$$\text{flux of } [E^-] \text{ out} = \text{flux of } [OH^-] \text{ in} + \text{flux of } [H^+] \text{ out} \quad (\text{Eq. 6})$$

4. The value of J_{OH} , as well as of J_E and J_H , can be calculated at any given point in the diffusion layer by using Fick's first law of diffusion (15). Then, when $[OH^-]$ flux calculated by this means was found to be equal to the value obtained using Eq. 6, the boundary condition for $[OH^-]$ was defined. Thus:

$$D_{OH} \frac{d[OH^-]}{dX} = \text{flux of } [E^-] - \text{flux of } [H^+] \quad (\text{Eq. 7})$$

5. The boundary condition for $[H^+]$ at the wall was given by the equilibrium relationship between $[OH^-]$ and $[H^+]$ (Eq. 5).
6. Since the bulk concentrations for E^- and K were very low, they were considered to be zero (initial rates were assumed). The boundary conditions at $X = h$ for $[OH^-]$ and $[H^+]$ were given by the bulk pH. Thus, all boundary conditions required for the simulation of phenylbutazone dissolution were set. These conditions are summarized here.

At $X = 0$:

$$[K]_0 = \text{solubility of HA}$$

$$[E^-]_0; J_{\text{obs}} = J_K + J_E$$

$$[OH^-]_0; D_{OH} \frac{d[OH^-]}{dX} = J_E - J_H$$

$$[H^+]_0 = \frac{K_w}{[OH^-]_0}$$

At $X = h$:

$$[K]_h = 0$$

$$[E^-]_h = 0$$

$$[OH^-]_h = \text{from bulk pH}$$

$$[H^+]_h = \text{from bulk pH}$$

To solve the two-point value problem, conditions on each side of the boundary must be specified. This was not the case in these simulations. One alternative was to guess the initial slopes at one boundary and to solve the problem as an initial value problem "shooting" repeatedly at the other boundary until the known boundary conditions were satisfied (16, 17). Since this approach was costly and time consuming, a second

² Ciba-Geigy Pharmaceuticals, Summit, N.J.

³ Aldrich Chemical Co., Milwaukee, Wis.

⁴ Fisher Scientific Co., Fair Lawn, N.J.

⁵ Model 219, Cary Instruments, Calif.

approach was taken where the dissolution of phenylbutazone was simulated assuming steady-state conditions. The nonsteady-state solution continued until steady state was achieved. It was necessary to establish four initial conditions besides the eight boundary conditions already described to solve the system as a nonsteady-state problem.

Thus, the initial conditions for phenylbutazone and all of the diffusing species were given by, at $t = 0$:

$$\begin{aligned} [K]_0 &= \text{solubility of } [HA]_0 \\ [OH^-]_0 &= \text{from bulk pH} \\ [H^+]_0 &= \text{from bulk pH} \\ [E^-]_0 &= 0 \end{aligned}$$

The mathematical model representative of phenylbutazone dissolution was represented by a set of four nonlinear partial differential equations (Eqs. 1-4), which could be written in finite difference forms.

Let the diffusion layer be divided into M grid points denoted by X_i , $i = 1, 2, \dots, M$. The time index was given by the subscript n , where $n + 1$ is the new time and n is the old time.

The left side of Eqs. 1-4 written in finite-difference approximation by:

$$\frac{\partial [N]}{\partial t} = \frac{[N]_{i,n+1} - [N]_{i,n}}{\Delta t} \quad (\text{Eq. 8})$$

where N represents any of the species, K , E^- , OH^- , or H^+ . The right side of Eqs. 1-4 can be written in terms of the Crank-Nicolson (15, 18) implicit finite-difference formulation, around the node i , as follows:

$$\frac{\partial^2 [N]}{\partial X^2} = \frac{D_N}{2} \delta_X^2 [N]_{i,n+1} + \frac{D_N}{2} \delta_X^2 [N]_{i,n} - (\text{kinetic term})_{i,n+1} \quad (\text{Eq. 9})$$

where:

$$\delta_X^2 [N]_{i,n+1} = \frac{[N]_{i-1,n+1} - 2[N]_{i,n+1} + [N]_{i+1,n+1}}{(\Delta X)^2} \quad (\text{Eq. 10})$$

$$\delta_X^2 [N]_{i,n} = \frac{[N]_{i-1,n} - 2[N]_{i,n} + [N]_{i+1,n}}{(\Delta X)^2} \quad (\text{Eq. 11})$$

where D_N is the diffusivity of the particular N species being considered.

As shown by the preceding equations, the kinetic terms impose nonlinear characteristics to the system. If it is assumed that these kinetic terms are considered at time n instead of time $n + 1$, the solution of these equations becomes available by using a Crank-Nicolson technique. This assumption causes no great deviation compared to the results obtained using the shooting method.

When Eqs. 1-4, expressed by finite-difference approximations, were applied to the various grid points in the diffusion layer, a set of $M - 1$ linear equations resulted at each time step. The coefficients formed a tridiagonal matrix, which could be solved by a Gaussian elimination technique (19) with a maximum of three variables per equation.

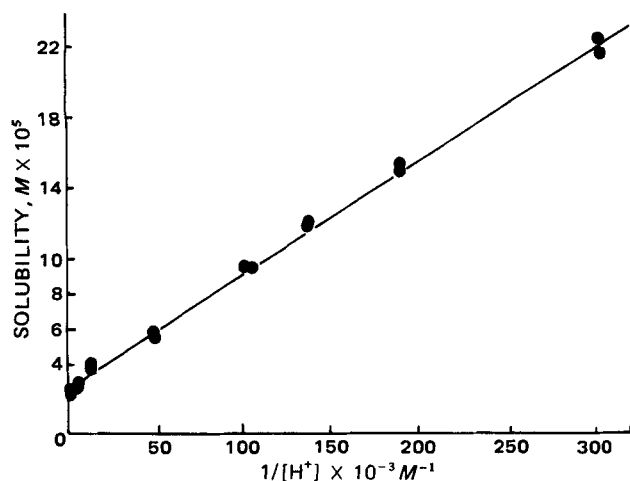


Figure 1—Plot of the aqueous solubility of phenylbutazone versus $1/[H^+]$ (25° at $\mu = 0.5$ with potassium chloride).

After solving the system for $[N]_{i,n+1}$ at the next iteration, the process was tested for convergence at every grid node:

$$\frac{\text{abs}[\Delta [N]_{i,n+1} - \Delta [N]_{i,n}]}{\text{abs} \Delta [N]_{i,n+1}} < \text{convergence}$$

where $\Delta [N]_i$ was the difference of $[N]$ between two grid points, and the value of tolerance was specified.

The Crank-Nicolson method was stable for all values of the ratio $\lambda = \Delta t / (\Delta X)^2$ for linear equations. However, this system was not linear. When a small Δt was used, the amount of computation was large. For the case of $\lambda < 4000$, the system was stable but convergence was reached over a longer period. When $\lambda > 20,000$, the system became unstable. Finally, when $\lambda = 4000$, the system converged rapidly, saving computation time.

RESULTS AND DISCUSSION

The solubility of phenylbutazone was measured as a function of the reciprocal of the hydrogen-ion concentration ($1/[H^+]$) in 0.1 M acetate buffers ($\mu = 0.5$ with potassium chloride). The results are plotted in Fig. 1. The intrinsic solubility of undissociated phenylbutazone species, $[HA]_0$, and the macroscopic dissociation constant, K_a , are related to the total solubility (S) of phenylbutazone by:

$$S = [HA]_0 + \frac{K_a [HA]_0}{[H^+]} \quad (\text{Eq. 12})$$

By plotting S versus $1/[H^+]$, a straight-line relationship gives $[HA]_0$ as the intercept and $([HA]_0 K_a)$ as the slope. Dividing the slope by the intercept gives K_a , which is the macroscopic dissociation constant for phenylbutazone (3).

The pKa of phenylbutazone determined by spectrophotometry may be given by:

$$\text{pKa} = \text{pH} + \log \frac{A_{\text{base}} - A_{\text{obs}}}{A_{\text{obs}} - A_{\text{acid}}} \quad (\text{Eq. 13})$$

where pKa is the macroscopic value measured at $\mu = 0.5$ with potassium chloride, A_{base} is the absorbance of a given solution of phenylbutazone under basic conditions where the phenylbutazone is virtually 100% in its anion form, A_{acid} is the absorbance of the same solution under acidic conditions where phenylbutazone exists essentially as 100% in the protonated form, and A_{obs} is the absorbance of the same solution at a pH between the two extremes (denoted as pH in Eq. 13). The pKa values of phenylbutazone under these experimental conditions were 4.61 (solubility technique) and 4.54 (spectrophotometric technique), and the intrinsic solubility was $2.61 \times 10^{-5} M$.

Deuteration of Phenylbutazone and 2-Naphthoic Acid—IR and NMR studies of the deuterated and nondeuterated forms of phenylbutazone and 2-naphthoic acid showed conclusively that the acidic proton of the nondeuterated forms was exchanged for deuterium and that no other protons in the molecules were affected. NMR spectra of both pairs of compounds showed the disappearance of the acidic proton signal (δ 12.5 ppm for 2-naphthoic acid⁶ and 3.2 ppm for phenylbutazone⁷ with reference to a tetramethylsilane standard). On deuteration, no other differences in the NMR spectra were observed.

IR spectra of both forms of phenylbutazone were very similar except for a sharpening of a peak at 2860 cm^{-1} and the presence of additional peaks at 2060 cm^{-1} and $1100\text{--}1200 \text{ cm}^{-1}$ for the deuterated form. The IR spectra for both forms of 2-naphthoic acid showed a more noticeable difference between the compounds. The broad band, typically associated with intermolecular hydrogen bonding ($2200\text{--}2100 \text{ cm}^{-1}$), was present in the spectrum of the protonated form but virtually absent in that of the deuterated form. This finding suggested that the lower melting point of the deuterated 2-naphthoic acid ($180\text{--}181^\circ$) compared to that of the protonated form ($184\text{--}185^\circ$) was due to a significantly lower degree of hydrogen (or deuterium) bonding in the deuterated 2-naphthoic acid.

Initial Dissolution Rates as a Function of Disk Rotation Speed—Table I shows the initial dissolution rates of phenylbutazone as a function of disk rotation speed in solutions of $\text{pH}_{\text{bulk}} 2.0$ and 6.50 and of *d*-phenylbutazone as a function of the same disk rotation speeds at $\text{pH}_{\text{bulk}} 6.50$. These data are plotted versus $\omega^{1/2}$ (a function of rotation speed) in Fig. 2. Table II shows the initial dissolution rates of 2-naphthoic acid and *d*-2-naphthoic acid in a solution of $\text{pH}_{\text{bulk}} 2.0$ at varying disk

⁶ Solvent used was deuterated chloroform-dimethyl sulfoxide- d_6 , $\sim 1:2$.

⁷ Solvent used was carbon tetrachloride with tetramethylsilane standard in deuterated chloroform.

Table I—Initial Dissolution Rates (J_{obs}) of Phenylbutazone and *d*-Phenylbutazone at Varying Disk Rotation Speeds in Media of $\mu = 0.5$ with Potassium Chloride and Varying pH_{bulk} at 25°

| Disk Rotation Speed, rpm | $\omega^{1/2a}$ | Phenylbutazone | | <i>d</i> -Phenylbutazone, |
|--------------------------|-----------------|---|---|---|
| | | $J_{obs} (\pm SD)^b$ (at pH_{bulk} 2.00^c) $\times 10^5$ | J_{obs}^b (at pH_{bulk} 6.5^d) $\times 10^5$ | J_{obs}^b (at pH_{bulk} 6.5^d) $\times 10^5$ |
| 100 | 3.24 | 1.23 (± 0.26) | 3.68 | 3.04 |
| 200 | 4.58 | 1.66 (± 0.04) | 4.74 | 3.66 |
| 300 | 5.61 | 1.80 (± 0.17) | 5.88 | 4.32 |
| 450 | 6.87 | 2.04 (± 0.12) | 6.64 | 4.94 |
| 600 | 7.93 | 2.58 (± 0.34) ^e | 7.24 | 5.66 |
| 900 | 9.71 | — | 8.67 | 6.50 |

^a The angular velocity of the disk in radians per second. ^b The standard deviation is from at least four measurements; where standard deviation values are not given, the mean was obtained from two or three similar values. (The J units are $mg\ cm^{-2}/sec$ and not $moles\ cm^{-2}/sec$). ^c In 0.01 *M* HCl/0.49 *M* KCl solution. ^d In 0.5 *M* KCl solution, pH-statted. ^e *d*-Phenylbutazone under these conditions gave an initial dissolution rate of $2.98 \times 10^{-5} (\pm 0.23 \times 10^{-5})\ mg\ cm^{-2}/sec$.

Table II—Initial Dissolution Rates (J_{obs}) of 2-Naphthoic and *d*-2-Naphthoic Acids at Varying Disk Rotation Speeds in Media of $\mu = 0.5$ with Potassium Chloride and pH_{bulk} 2.00^a at 25°

| Rotation Speed, rpm | $\omega^{1/2c}$ | $J_{obs} (\pm SD)^b$ (at pH_{bulk} 2.00 $\times 10^5$) | |
|---------------------|-----------------|--|----------------------------|
| | | 2-Naphthoic Acid | <i>d</i> -2-Naphthoic Acid |
| 100 | 3.24 | 3.63 (± 0.09) ^d | 3.71 (± 0.13) |
| 200 | 4.58 | 4.88 (± 0.06) | 4.87 (± 0.13) |
| 300 | 5.61 | 5.78 (± 0.05) | 5.74 (± 0.17) |
| 450 | 6.87 | 7.37 (± 0.47) | 7.32 (± 0.48) |
| 600 | 7.93 | 8.52 (± 0.52) | 8.40 (± 0.18) |
| 900 | 9.71 | 10.09 (± 0.57) | 10.01 (± 0.36) |

^a Medium was 0.01 *M* HCl/0.49 *M* KCl with no pH-stat used during dissolution runs. ^b The standard deviation from three repeated runs. ^c The angular velocity of the disk in radians per second. ^d All units are in $mg/cm^2/sec$.

rotation speeds. These data were not plotted because they are essentially identical to those given previously (1). All the dissolution rate data as a function of rotation speed are summarized in Table III.

The Levich-Nernst model states that J , the dissolution rate from a rotating disk of solid material, is directly proportional to $\omega^{1/2}$, a function of the disk's rotation speed, as seen by:

$$J = 0.62 D^{2/3} \nu^{-1/6} C_S \omega^{1/2} \quad (\text{Eq. 14})$$

where D is the diffusivity of the dissolving solute, ν is the kinematic viscosity of the dissolution medium, C_S is the saturated solubility of the dissolving solute in the medium, and ω is the angular velocity of the rotating disk in radians per unit time. From Fig. 2, phenylbutazone under acidic conditions appeared to show a reasonable degree of linearity when J was plotted against $\omega^{1/2}$. Therefore, phenylbutazone dissolves by a diffusion layer-controlled mechanism under acidic conditions since the correlation coefficient for this plot was reasonable and the calculated diffusivity from these data ($4.90 \times 10^{-6}\ cm^2/sec$) was very close to that obtained from the square root relationship previously discussed (1) using the diffusivity of benzoic acid under identical conditions as a standard.

Table III—Summary of Data Obtained for Protonated and Deuterated Forms of 2-Naphthoic Acid and Phenylbutazone from the J_{obs} versus $\omega^{1/2}$ Regression Analysis (Data in Tables I and II) Performed at Varying pH_{bulk} and 25°

| Compound | pH_{bulk} | Slope of J_{obs} versus $\omega^{1/2}$ $\times 10^6$ | Intercept of J_{obs} versus $\omega^{1/2}$ $\times 10^5$ | Correlation Coefficient for r | Diffusivity from Slope, $(cm^2/sec) \times 10^6$ |
|----------------------------|-------------|---|---|---------------------------------|--|
| 2-Naphthoic acid | 2.00 | 10.44 | 0.01 | 0.9991 | 6.52 ^a |
| <i>d</i> -2-Naphthoic acid | 2.00 | 10.30 | 0.01 | 0.9989 | 6.39 ^a |
| Phenylbutazone | 2.00 | 3.07 | 0.10 | 0.9792 | 4.80 ^b |
| Phenylbutazone | 6.50 | 7.59 | 1.34 | 0.9961 | — |
| <i>d</i> -Phenylbutazone | 6.50 | 5.46 | 1.23 | 0.9975 | — |

^a Calculated from Levich relationship (Eq. 14) and $[HA]_0 = 2.23\ mg/ml$ in $\mu = 0.5$ with potassium chloride. ^b Calculated from Levich relationship (Eq. 14) and $[HA]_0 = 8.1 \times 10^{-2}\ mg/ml$.

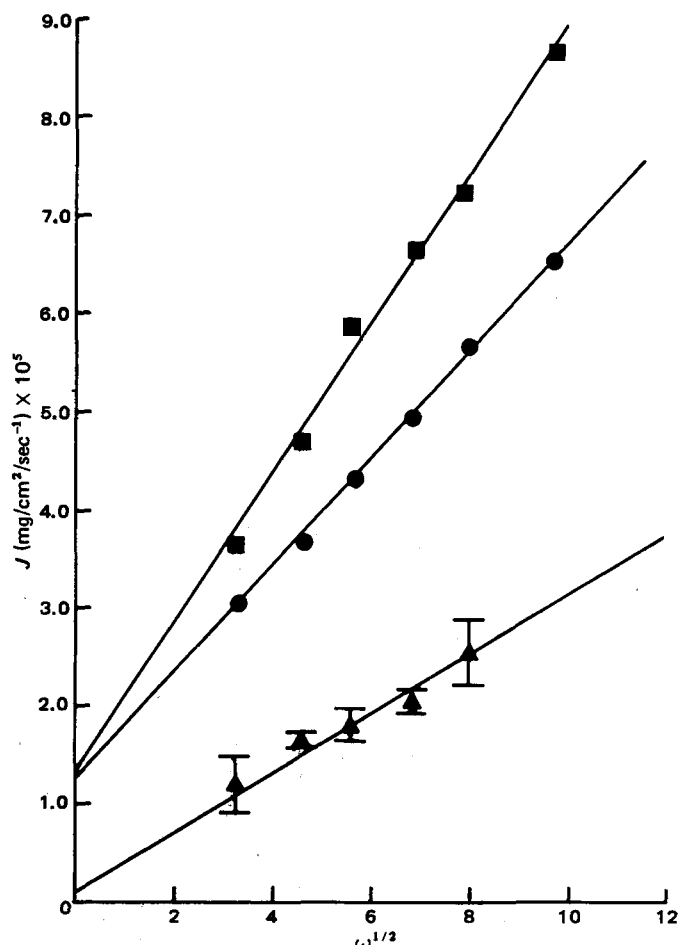


Figure 2—Levich plot of the dissolution rate (J) as a function of the square root of the angular velocity ($\omega^{1/2}$) of a rotating disk of phenylbutazone (\blacksquare) and *d*-phenylbutazone (\bullet) at pH 6.5 (maintained by a pH-stat) and of phenylbutazone (\blacktriangle) at pH 2.0 (25° at $\mu = 0.5$ with potassium chloride).

Initial dissolution rates of phenylbutazone and *d*-phenylbutazone with varying rotation speed at pH_{bulk} 6.50 did not strictly obey the Levich model but showed the type of behavior that indomethacin displayed in earlier work under similar conditions (1). An additional mechanism appeared to be contributing to the dissolution rate of pH_{bulk} 6.50, which was independent of the disk rotation speed as shown by a nonzero intercept.

It was assumed that a modified form of the Levich-Nernst relationship applies:

$$J = (0.62 D^{2/3} \nu^{-1/6} C_S) \omega^{1/2} + \text{constant} \quad (\text{Eq. 15})$$

where the constant represents the nonzero intercept at zero rotation speed. The cause of this nonzero intercept is unknown but is being studied.

Table IV—Absolute Dissolution Rates from Rotating Disks of Phenylbutazone and *d*-Phenylbutazone (600 rpm) as a Function of Bulk Solution pH^a

| pH _{bulk} | pH ₀ (at X = 0) | J _{obs} ^H | J _{obs} ^D | J _{theor} ^H |
|--------------------|-------------------------------|-------------------------------|-------------------------------|---------------------------------|
| 2.00 | 2.00 | 8.35 | 10.12 | 8.10 |
| 3.00 | 3.00 | 6.53 | — | 8.28 |
| 4.00 | 4.00 | 9.42 | 8.74 | 10.04 |
| 4.50 | 4.46 | — | 11.95 | 13.78 |
| 5.00 | 4.78 | 19.95 | 11.25 | 20.01 |
| 5.50 | 4.91 | — | 16.06 | 24.36 |
| 6.00 | 4.96 | — | 17.92 | 26.12 |
| 6.50 | 4.97 | — | 19.83 | 26.74 |
| 7.00 | 4.98 | 27.18 | 20.27 | 27.00 |
| 8.00 | 5.00 | 28.26 | 22.03 | 27.91 |
| 8.50 | 5.05 | 30.34 | 24.46 | 30.06 |
| 9.00 | 5.18 | 38.34 | 32.95 | 38.07 |
| 9.20 | 5.28 | 49.53 | — | 46.11 |
| 9.50 | 5.50 | 78.76 | 68.25 | 70.90 |
| 9.70 | 5.68 | 110.29 | — | 102.40 |
| 10.00 | 5.96 | 165.03 | 169.97 | 190.67 |
| 10.20 | 6.16 | 297.75 | — | 295.60 |

^a J_{theor}^H is the calculated flux, assuming phenylbutazone acts as a classical acid; J_{obs}^H is the observed flux of phenylbutazone; and J_{obs}^D is the observed flux of *d*-phenylbutazone. All values of J are in units of moles cm⁻²/sec × 10¹¹.

The two forms of phenylbutazone did not dissolve at the same rate at a given disk rotation speed at pH_{bulk} 6.5, with *d*-phenylbutazone dissolving more slowly than phenylbutazone. Although *d*-phenylbutazone dissolution rates were not extensively measured under acidic conditions, a value was determined at 600 rpm at pH_{bulk} 2.00, and it did not differ significantly from that obtained for phenylbutazone under the same conditions. Hence, the difference in dissolution rates of these compounds at pH_{bulk} 6.50 may be due to a difference in the ionization rates of the two species within the diffusion layer.

The dissolution rates of 2-naphthoic acid and *d*-2-naphthoic acids under acidic conditions as a function of disk rotation speed showed that there was no significant difference between the two compounds when ionization was suppressed during the dissolution process. Thus, it was assumed that the deuteration of 2-naphthoic acid did not affect the intrinsic solubility of the acid, despite differences in crystal lattice energies (assumed from the melting point data) being observed between the dissolving solids. In view of the lability of deuterium bonded to a carboxylic acid oxygen atom, the similarity between results obtained for the dissolution rates of the two forms of 2-naphthoic acid was probably due to rapid exchange of deuterium with hydrogen in water immediately at the solid-liquid interface during dissolution. Thus, the diffusion rate of the nondeuterated form away from the solid-liquid interface was observed in both cases.

Initial Dissolution Rates as Function of pH_{bulk}—Tables IV and V contain initial dissolution rate data for both deuterated and protonated forms of phenylbutazone and 2-naphthoic acid as a function of pH_{bulk} (maintained by pH-stat) and at a constant rotation speed. Also included are the theoretical values expected if 2-naphthoic acid and phenylbutazone acted as classical acids, ionizing instantaneously as they diffused through the diffusion layer (1).

Adherence of the dissolution rates of 2-naphthoic acid to the model

Table V—Absolute Dissolution Rates from Rotating Disks of 2-Naphthoic Acid (450 rpm) as a Function of Bulk pH^a

| pH _{bulk} | pH ₀ (X = 0 from theory) | J _{theor} ^H (moles cm ⁻² /sec) × 10 ¹⁰ | J _{obs} ^H (moles cm ⁻² /sec) × 10 ¹⁰ | J _{obs} ^D (moles cm ⁻² /sec) × 10 ¹⁰ |
|--------------------|---|---|---|---|
| 2.00 | 2.00 | 3.950 | 4.280 | 4.249 |
| 6.00 | 4.28 | 11.130 | 13.300 | 13.547 |
| 7.00 | 4.29 | 11.200 | 13.820 | 13.853 |
| 8.00 | 4.29 | 11.270 | 13.590 | 13.754 |
| 8.50 | 4.30 | 11.430 | 14.170 | 14.056 |
| 9.00 | 4.33 | 11.940 | 14.990 | 15.305 |
| 9.20 | 4.35 | 12.400 | 16.150 | 16.561 |
| 9.50 | 4.42 | 13.760 | 18.240 | 18.683 |
| 10.00 | 4.49 | 22.560 | 27.360 | 26.520 |

^a J_{theor}^H is the calculated mass transport rate, J_{obs}^H is the observed flux of the protonated acid, and J_{obs}^D is the observed flux of the deuterated acid.

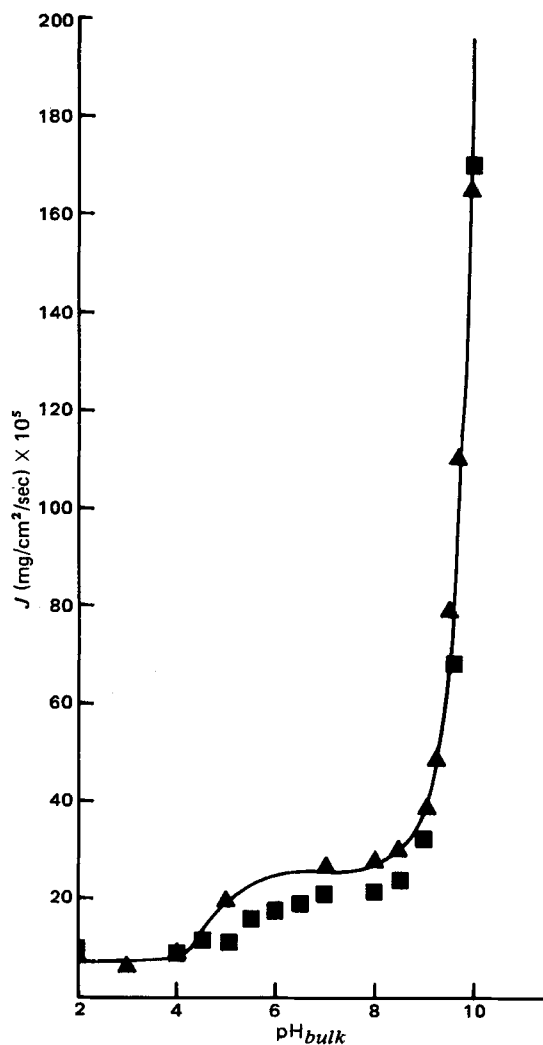


Figure 3—Dissolution rate (J) versus pH_{bulk} profile for phenylbutazone (▲) and *d*-phenylbutazone (■) from a rotating disk (600 rpm) dissolving in an aqueous medium (25° at μ = 0.5 with potassium chloride). The pH_{bulk} was maintained with a pH-stat. The continuous line represents the profile generated treating phenylbutazone as a carboxylic acid.

described earlier (1), assuming instantaneous chemical-ionization reactions within the diffusion layer, was already established. Since the values for 2-naphthoic acid and the *d*-2-naphthoic acid (J_{obs}^D) closely agreed at every pH_{bulk} value tested and since these values approximated those predicted by theory (J_{theor}), it may be reasoned that the deuterated and nondeuterated forms of 2-naphthoic acid diffuse and simultaneously react with base in the same way and to the same extent. This reasoning also confirmed that the two compounds dissolved and instantaneously achieved equilibrium with the reacting base in the diffusion layer and, therefore, acted in a classical manner. This behavior was consistent with the more rapid exchange of deuterium for hydrogen relative to the time taken for the molecules to traverse the diffusion layer. If exchange occurred instantaneously for the *d*-2-naphthoic acid at the solid-liquid interface, then it should dissolve identically to 2-naphthoic acid.

The data for deuterated and nondeuterated phenylbutazone (Table IV and Fig. 3) may be compared in the same way as for 2-naphthoic acid. Comparison between the J_{obs} values for the two phenylbutazone forms to the J_{theor} values for the same pH_{bulk} showed that the fluxes of *d*-phenylbutazone were significantly slower than those of phenylbutazone by ~10–45% over the neutral pH_{bulk} range. Furthermore, phenylbutazone gave experimental dissolution rates very close in value to those predicted by the theory (1) that assumed instantaneous equilibrium. Therefore, at 25° and μ = 0.5 with potassium chloride and over a wide range of bulk solution pH, phenylbutazone was an example of a compound dissolving into a reactive medium showing simultaneous noninstantaneous chemical reaction that could be treated as if its ionization was instantaneous; i.e.,

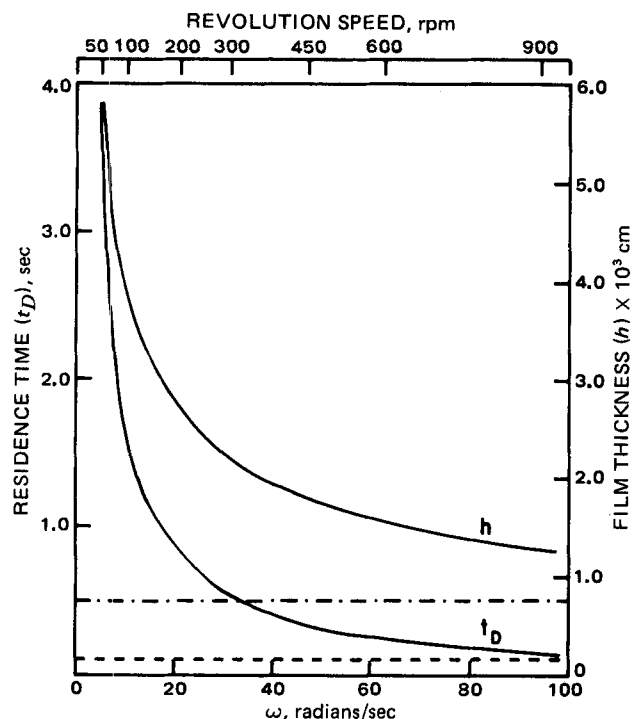


Figure 4—Plot of residence time (t_D) and apparent diffusion layer thickness (h) for phenylbutazone as defined by Eqs. 18 and 19 versus ω (angular velocity) for dissolution from a rotating disk. Times are shown for three half-lives for the deprotonation reaction (at $\text{pH}_{\text{bulk}} 6.5$). Key: ---, phenylbutazone, and - - -, *d*-phenylbutazone.

the experimental results suggested that the ionization was still rapid enough that, relative to the diffusional processes, phenylbutazone still acted classically.

Contrary to the results shown for deuterated and nondeuterated 2-naphthoic acids, *d*-phenylbutazone dissolution between $\text{pH}_{\text{bulk}} 5.00$ and 9.00 was markedly slower than that of phenylbutazone. It was thought that by studying *d*-phenylbutazone, where deuterium was exchanged for hydrogen at the ionizing center of the phenylbutazone molecule, any effects on its dissolution rate in reactive media due to the noninstantaneous ionization kinetics of phenylbutazone would be amplified. The rationale for this approach was explained earlier (12) and was based on the comparative strengths of a C–D and a C–H bond, a greater free energy of activation (ΔG^\ddagger) being required to break the C–D bond for ionization than that required in the breaking of the C–H bond. Hence, the values of k_1 and k_3 in Schemes I and II should be smaller for *d*-phenylbutazone, whereas k_2 and k_4 should remain the same as in phenylbutazone if it is assumed that the reverse reaction, once the deuterium is removed, involves only protons.

Residence Time and Ionization Reaction Time in Diffusion Layer—When phenylbutazone diffuses across the aqueous diffusion layer during dissolution in an unreactive medium (*i.e.*, under acidic

conditions) under steady-state conditions, the concentration profile for the acid will be linear as given by the Nernst model (1). Higuchi *et al.* (20) demonstrated that, under these conditions, the residence time (t_D), which was the average lifetime of a diffusing molecule in the diffusion layer of thickness h , was inversely proportional to the diffusivity of the molecule. The relationship between t_D , the diffusivity, and diffusion layer thickness is given by:

$$t_D = \frac{h^2}{2D_K} \quad (\text{Eq. 16})$$

where D_K is as previously described. Since an expression for h is given by the Levich rotating disk model shown by:

$$h = 1.612 D_K^{1/3} \nu^{1/6} \omega^{-1/2} \quad (\text{Eq. 17})$$

substitution for h may be performed in Eq. 16 to give:

$$t_D = \frac{1.3 \nu^{1/3}}{D_K^{1/3} \omega} \quad (\text{Eq. 18})$$

Thus, for the specific case of steady-state initial dissolution conditions from a rotating disk, Eq. 18 states that t_D is inversely proportional to ω , the angular velocity of the disk in radians per unit time.

Figure 4 shows a plot of residence time and diffusion layer thickness versus ω for phenylbutazone, assuming that no chemical reaction occurs during the dissolution process (calculated from parameter values previously determined). For convenient representation of the relationship between t_D , h , and rotation speed, the abscissa is also marked in revolutions per minute (directly proportional to ω).

When phenylbutazone was dissolving into a medium of pH greater than its pK_a , it would tend to dissociate according to the pH of the diffusion layer. With classical acids, this dissociation process was instantaneous, as described for 2-naphthoic acid. For a carbon acid such as phenylbutazone, however, the observed rate constant for the rate of approach to this equilibrium can be slow (3).

Astarita (21) defined a reaction time (t_r) that is similar to the half-life in a first-order or pseudo-first-order reaction and is given by:

$$t_r = \frac{1}{k} \quad (\text{Eq. 19})$$

where k is a simple first-order or pseudo-first-order rate constant defining the reaction process. Therefore, the t_r value represents the time taken to complete 63% of the given reaction by a first-order mechanism.

If the given average reaction time was much longer than the average residence time of phenylbutazone in the diffusion layer under defined hydrodynamic conditions, the reaction would only effectively take place in the bulk solution. As the reaction time (t_r) decreased to where it became closer in value to t_D , the dissociation reaction would influence the flux as defined by Eqs. 1–4. Once t_r becomes much smaller than t_D , phenylbutazone should behave classically, *i.e.*, as in the case of 2-naphthoic acid.

Phenylbutazone ionization kinetics cannot normally be represented by a simple overall first-order process (3). Stella and Pipkin (3) described an equation for calculating the observed buffer-independent rate constant for approach to the ionization equilibrium (Eq. 20) for phenylbutazone and specified conditions under which it may be simplified.

$$k_{\text{obs}} = k_1 + k_3[\text{OH}^-] + \frac{k_2[\text{H}^+]K_{a,\text{enol}}}{K_{a,\text{enol}} + [\text{H}^+]} + \frac{k_4 K_{a,\text{enol}}}{K_{a,\text{enol}} + [\text{H}^+]} \quad (\text{Eq. 20})$$

where k_{obs} is the rate constant for the approach to equilibrium, k_{1-4} are

Table VI—Calculated k_{obs} and (t_r) across the Diffusion Layer of Phenylbutazone Dissolving in $\text{pH}_{\text{bulk}} 6.50$ Using a pH-stat at $\mu = 0.5$ and 25°

| Fractional Distance across Film (x/h) ^a | pH_X | $[\text{OH}^-]_X$ ^b , M | $[\text{H}^+]_X$ ^b , M | k_1 ^c , sec ⁻¹ | $\left(\frac{k_2[\text{H}^+]_X K_{a,\text{enol}}}{K_{a,\text{enol}} + [\text{H}^+]_X}\right)$ ^c | k_{obs} ^d , sec ⁻¹ | $t_r = 1/k_{\text{obs}}$ ^d , $\times 10^2$ sec |
|--|---------------|------------------------------------|-----------------------------------|--|--|---|---|
| 0 | 4.97 | 9.42×10^{-10} | 1.06×10^{-5} | 10.1 | 2.24 | 12.34 | 8.10 |
| 0.2 | 5.05 | 1.12×10^{-9} | 8.96×10^{-6} | 10.1 | 1.89 | 11.99 | 8.34 |
| 0.4 | 5.15 | 1.40×10^{-9} | 7.16×10^{-6} | 10.1 | 1.51 | 11.61 | 8.61 |
| 0.6 | 5.29 | 1.93×10^{-9} | 5.18×10^{-6} | 10.1 | 1.09 | 11.19 | 8.94 |
| 0.8 | 5.53 | 3.41×10^{-9} | 2.93×10^{-6} | 10.1 | 0.62 | 10.72 | 9.33 |
| 1.0 | 6.50 | 3.16×10^{-8} | 3.16×10^{-7} | 10.1 | 0.07 | 10.17 | 9.94 |

^a Actual value of $h = 1.59 \times 10^{-3}$ cm. ^b Phenylbutazone is treated as a classical acid. ^c k_1 , k_2 , and $K_{a,\text{enol}}$ from Ref. 3. ^d Defined by Eq. 21.

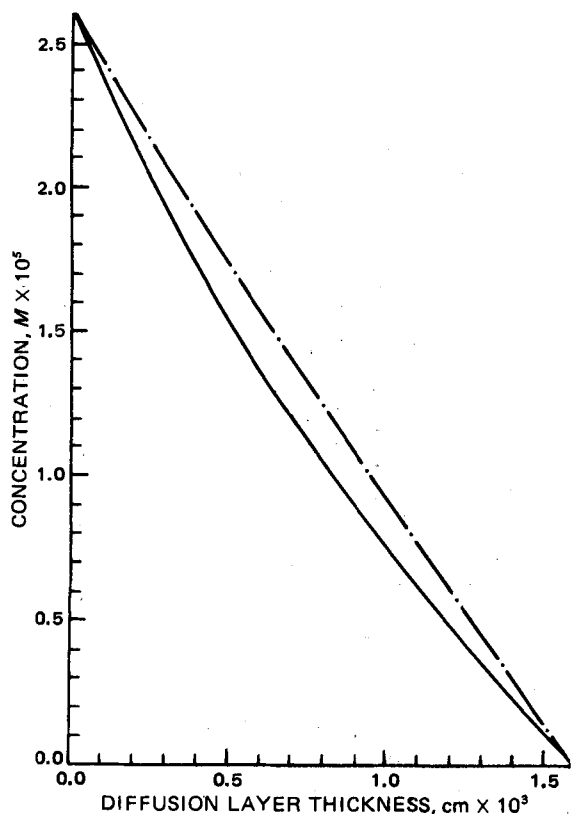


Figure 5—Concentration profiles across an aqueous diffusion layer for phenylbutazone (—) and d-phenylbutazone (---) at $\text{pH}_{\text{bulk}} 5$.

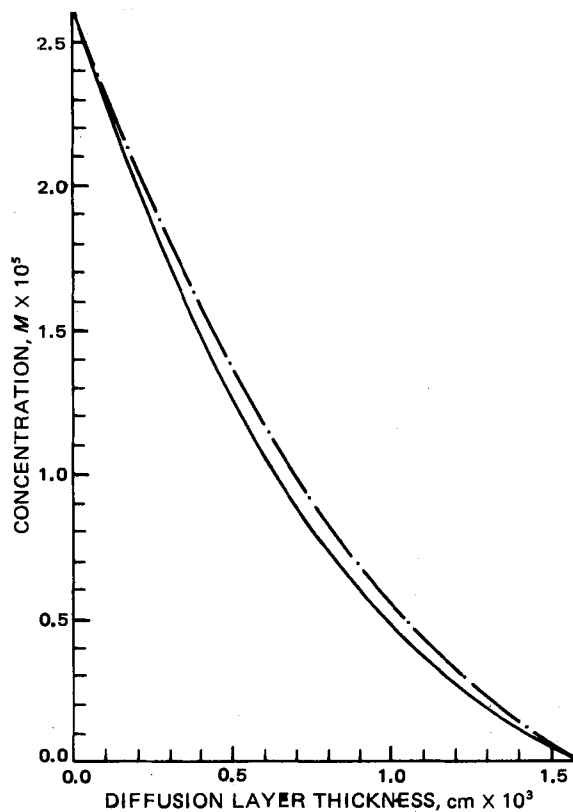


Figure 7—Concentration profiles across an aqueous diffusion layer for phenylbutazone (—) and d-phenylbutazone (---) at $\text{pH}_{\text{bulk}} 9$.

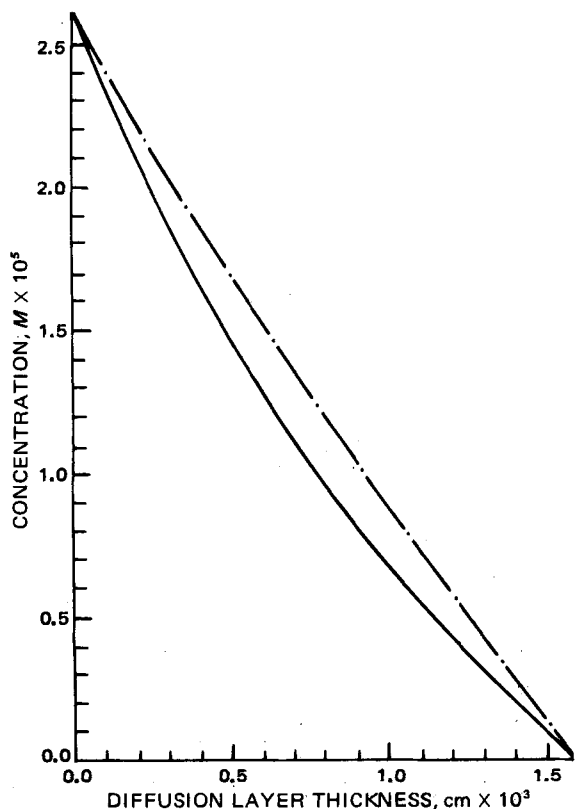


Figure 6—Concentration profiles across an aqueous diffusion layer for phenylbutazone (—) and d-phenylbutazone (---) at $\text{pH}_{\text{bulk}} 7$.

as given previously, $[\text{H}^+]$ is the hydrogen-ion concentration, $[\text{OH}^-]$ is the hydroxide-ion concentration at which k_{obs} is determined, and $K_{a,\text{enol}}$ is the dissociation constant of the enolic form of phenylbutazone (3). Although all of the data for these parameters were measured at $\mu = 0.1$ and 25° (3), it will be assumed that the values would remain reasonably unchanged in a medium of ionic strength 0.5.

From the phenylbutazone dissolution data measured in $\text{pH}_{\text{bulk}} 6.50$ using varying rotation speeds and Eq. 20, it was possible to gain some insight into the approximate values of k_{obs} within the diffusion layer during dissolution. Since the nondeuterated phenylbutazone dissolved in a classical manner in reactive media, the model used for instantaneous reaction (1) may be applied to phenylbutazone to estimate $[\text{H}^+]$ and $[\text{OH}^-]$ across the diffusion layer for any given bulk solution conditions.

Accordingly, $\text{pH}_{\text{bulk}} 6.50$ at 600 rpm was chosen and the values of $[\text{OH}^-]$, $[\text{H}^+]$, and pH in the diffusion layer was calculated using the instantaneous reaction model (1). From these values, it was possible to use a simplified version of Eq. 20 to calculate the corresponding values for k_{obs} at each point in the diffusion layer. The simplified form of Eq. 20 is given by:

$$k_{\text{obs}} = k_1 + \frac{k_2[\text{H}^+]K_{a,\text{enol}}}{K_{a,\text{enol}} + [\text{H}^+]} \quad (\text{Eq. 21})$$

which assumes from Eq. 20 that $k_3[\text{OH}^-]$ and k_4 are negligible relative to the other terms in the equation. Table VI shows the variation of k_{obs} across the film if the equilibrium values of $[\text{OH}^-]_X$ and $[\text{H}^+]_X$ actually exist at a given position X in the diffusion layer. Under these same conditions, t_D is 0.27 sec at 600 rpm.

The t_r values across the film do not differ by much and they approach the limiting value $t_r = 1/k_{\text{obs}} \approx 0.1$ sec. This value is displayed in the plot given in Fig. 4; assuming that the deviation from Levich-Nernst behavior seen at $\text{pH}_{\text{bulk}} 6.50$ in Fig. 2 is not significant, t_D only approaches the limiting t_r value when very rapid revolution speeds are used. Therefore, any effects that may be due to noninstantaneous ionization of phenylbutazone in the diffusion layer would only be significant when t_D approaches the value of t_r . Note that the limiting pH at $X = 0$ was ~ 5 . At this pH, the dissociation of phenylbutazone favors formation of its enolate anion. If t_r for establishing this equilibrium was longer or about the same as t_D

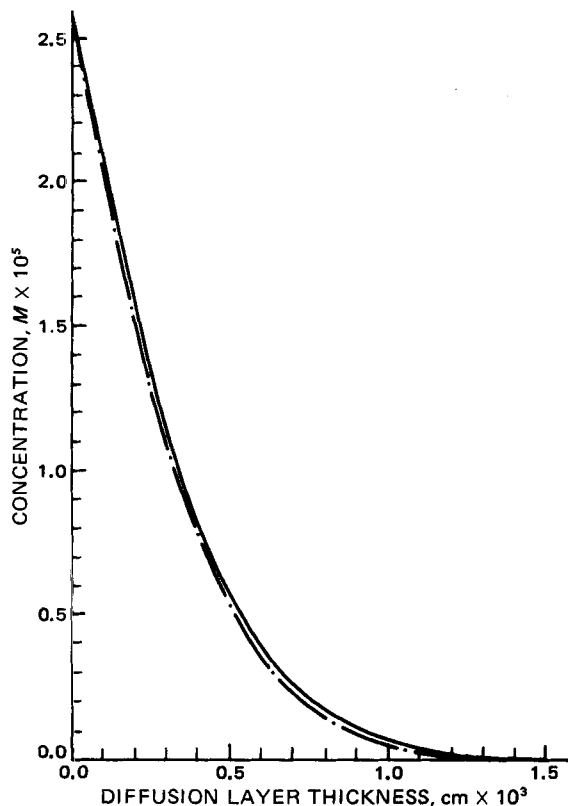


Figure 8—Concentration profiles across an aqueous diffusion layer for phenylbutazone (—) and *d*-phenylbutazone (---) at $\text{pH}_{\text{bulk}} 10$.

in the diffusion layer, then deviation from classical behavior should have been observed under the described conditions.

To support these statements, the behavior of *d*-phenylbutazone under identical conditions was studied. Deuterated phenylbutazone should show a slower rate of approach to equilibrium in its ionization due to a primary isotope effect; i.e., k_1 and k_3 for the initial dissociation of *d*-phenylbutazone will have a greater initial t_r value than phenylbutazone under the same conditions. Therefore, the rotation speed at which t_D becomes numerically similar to the limiting t_r value was expected to be lower for *d*-phenylbutazone than for phenylbutazone, assuming again that the Levich–Nernst model applied and there were no differences in D_{HA} and $[\text{HA}]_0$ between the two compounds.

The limiting t_r value of *d*-phenylbutazone may be approximated by assuming a value for the primary isotope effect for the deprotonation of phenylbutazone. If a primary isotope effect of five was assumed (22) in k_1 (ignoring k_3), a limiting t_r value of ~ 0.5 sec was calculated. This value was also displayed in Fig. 4 and indicated how t_D approaches the limiting value of t_r at much slower disk rotation speeds than in the case of phenylbutazone. Hence, any noninstantaneous reaction with base in the diffusion layer will affect the dissolution rates of *d*-phenylbutazone more than those of phenylbutazone under the same conditions. This finding was confirmed in Fig. 2 where the dissolution rates of *d*-phenylbutazone at $\text{pH}_{\text{bulk}} 6.50$ were significantly slower than those of phenylbutazone under identical conditions.

The qualitative arguments expressed here were useful in interpreting the differences in dissolution rates between phenylbutazone and *d*-phenylbutazone. Figures 5–8, obtained by integrating numerically Eqs. 1–4, show the concentration gradients existing across the diffusion layer during dissolution of phenylbutazone and its deuterio analog for pH 5, 7, 9, and 10. It was assumed in these simulations that *d*-phenylbutazone was dedeuterated by hydroxide ion and water five times slower than deprotonation of phenylbutazone. Calculated fluxes and pH at the interface are shown in Table VII.

The simulations appear to represent the flux data adequately. The observed dissolution rates for *d*-phenylbutazone were higher (pH 7 and 9) than the predicted theoretical values because deuterium was only abstracted once in practice but the model assumed that the rate of dissociation was that for deuterium for all abstractions. It can be seen from the figures that at pH 5 and 7, the concentration gradient between phe-

Table VII—Simulated (J_{theor}) and Observed (J_{obs}) Initial Dissolution Rates for Phenylbutazone and *d*-Phenylbutazone at Various pH_{bulk} Values ^a

| pH_{bulk} | $\text{pH}_0^{\text{calc } b}$ | Phenylbutazone | | <i>d</i> -Phenylbutazone | |
|---------------------------|--------------------------------|--------------------|------------------|--------------------------|------------------|
| | | J_{theor} | J_{obs} | J_{theor} | J_{obs} |
| 5 | 4.77 | 19.95 | 19.95 | 11.24 | 11.25 |
| 7 | 4.95 | 27.18 | 27.18 | 16.23 | 20.27 |
| 9 | 5.17 | 38.34 | 38.39 | 27.59 | 32.95 |
| 10 | 5.85 | 189.54 | 187.01 | 187.01 | 169.97 |

^a All values of J are in units of moles $\text{cm}^{-2}/\text{sec}$. ^b Calculated from the simulations.

nylbutazone and its deuterio analog was more marked than when these two compounds dissolved under more basic conditions. At pH 9, the gradient difference was smaller; at pH 10, it was negligible. These results were consistent with the earlier argument that as the pH_{bulk} is raised, the diffusion layer reaction time becomes faster and both phenylbutazone and *d*-phenylbutazone approach classical behavior ($t_r < t_D$). Thus, under neutral to slightly acidic conditions, deuterated phenylbutazone deviates from classical behavior. However, when basic conditions prevail, the dissolution of that compound was faster since the high concentration of hydroxide ion increased the rate of *d*-phenylbutazone ionization.

In view of the dissolution behavior of phenylbutazone under various conditions, it is unlikely that noninstantaneous ionization kinetics, demonstrated so clearly for this compound (3), play a major role in determining the dissolution rate, either *in vitro* or *in vivo*. This is due to the fact that the average diffusion layer residency time for a typical aqueous diffusion layer is longer than the average reaction time for the ionization of this carbon acid.

REFERENCES

- (1) K. G. Mooney, M. Mintun, K. J. Himmelstein, and V. J. Stella, *J. Pharm. Sci.*, **70**, 13 (1981).
- (2) *Ibid.*, **70**, 22 (1981).
- (3) V. J. Stella and J. D. Pipkin, *J. Pharm. Sci.*, **65**, 1161 (1976).
- (4) W. P. Jencks, "Catalysis in Chemistry and Enzymology," McGraw-Hill, New York, N.Y., 1969, pp. 175–178.
- (5) J. R. Jones, *Prog. Phys. Org. Chem.*, **9**, 244 (1972).
- (6) G. R. Van Petten, H. Feng, R. J. Whitney, and H. F. Lettau, *J. Clin. Pharmacol.*, **11**, 177 (1971).
- (7) R. J. Whitney, H. Feng, D. Cook, G. R. Van Peteten, and H. F. Lettau, *ibid.*, **11**, 187 (1971).
- (8) L. J. Lesson, "Proceedings of the Conference on Bioavailability of Drugs," B. B. Brodie and W. M. Heller, Eds., S. Karger, New York, N.Y., 1972, pp. 154–163.
- (9) *J. Am. Pharm. Assoc.*, NS16 p. 365 (1976).
- (10) E. G. Lovering and D. B. Black, *J. Pharm. Sci.*, **63**, 671 (1974).
- (11) *Ibid.*, **63**, 1399 (1974).
- (12) V. J. Stella, *J. Pharm. Sci.*, **64**, 706 (1975).
- (13) J. Matsunaga, N. Namju, and T. Nagai, *Chem. Pharm. Bull.*, **24**, 1169 (1976).
- (14) H. Ibrahim, F. Pisano, and A. Bruno, *J. Pharm. Sci.*, **66**, 669 (1977).
- (15) J. Crank and P. Nicolson, *Proc. Cambridge Philos. Soc.*, **43**, 50 (1947).
- (16) D. D. Morrison, J. D. Riley, and J. F. Zancanaro, *Commun. ACM*, **7**, 366 (1964).
- (17) J. F. Holt, *ibid.*, **5**, 613 (1962).
- (18) B. Carnahan, H. A. Luther, and J. O. Wilkes, "Applied Numerical Methods," Wiley, New York, N.Y., 1969, p. 451.
- (19) *Ibid.*, pp. 269–281.
- (20) T. Higuchi, H. K. Lee, and I. H. Pitman, *Farm. Aikak.*, **80**, 55 (1971).
- (21) G. Astarita, "Mass Transfer with Chemical Reaction," Elsevier, New York, N.Y., 1967, p. 9.
- (22) J. P. Klinman, in "Transition States of Biochemical Processes," R. D. Gandour and R. L. Schowen, Eds., Plenum, New York, N.Y. 1978, pp. 165–200.

ACKNOWLEDGMENTS

Adapted in part from a dissertation submitted by K. G. Mooney to the University of Kansas in partial fulfillment of the Doctor of Philosophy degree requirements.

Supported by National Institutes of Health Grant GM 22357.